INTERNATIONAL JOURNAL FOR NUMERICAL METHODS IN FLUIDS, VOL. 1, 63–79 (1981)

A SIMPLE METHOD TO GENERATE HIGH-ORDER ACCURATE CONVECTION OPERATORS FOR EXPLICIT SCHEMES BASED ON LINEAR FINITE ELEMENTS

J. DONÉA AND S. GIULIANI

Applied Mechanics Division, Joint Research Centre, Commission of the European Communities, Ispra Establishment, Italy

SUMMARY

A simple method is proposed to generate high-order accurate convection operators for lumped-explicit schemes based on linear or multilinear finite elements. The basic idea is to reduce the truncation error on the first-order spatial derivatives by exploiting the consistent mass matrix of the finite element method in a purely explicit multistep procedure. The effectiveness of the method is demonstrated on pure convection problems in one and two dimensions.

KEY WORDS Heat Transfer Convection Finite Element Method

INTRODUCTION

For the numerical solution of time-dependent convection dominated problems, conventional linear finite elements are much more accurate than standard second-order central difference methods. This is a direct consequence of the much improved phase characteristics associated with the consistent mass matrix of the finite element method. However, if an explicit scheme is chosen for time integration, mass lumping is virtually mandatory and one sacrifices the advantage of the consistent mass formulation. The deleterious effect of mass lumping on the quality of numerical solutions to pure convection problems has been illustrated in Gresho *et al.*[1] and Donéa *et al.*;[2] the main consequence is an overall phase error which manifests itself by the presence of spurious leading and trailing waves.

Since explicit algorithms may be cost-effective for solving large-scale convection dominated problems (see the excellent discussion by Cheng[3]), it appears worthwhile attempting to improve the phase characteristics of lumped-explicit finite element schemes. A possible strategy will be discussed in the present paper for the case of the basic isoparametric elements, i.e. the bilinear quadrilateral in two dimensions and the trilinear brick in three dimensions.

The poor phase characteristics of lumped-explicit schemes based on linear elements result from the severe truncation error on the first-order spatial derivatives introduced by the diagonal mass representation. To reduce this truncation error, it is proposed to exploit the consistent mass matrix of the finite element method in a purely explicit multistep procedure. The first step makes use of the diagonal mass representation to obtain a first approximation to the time rate of change of the nodal values of the computed quantity, while the successive steps yield improved approximations which are derived on the basis of an explicit use of the consistent mass matrix. On a uniform mesh of linear elements, the proposed multistep procedure is shown to generate an approximation to the first-order spatial derivative which is of order $2n$, n designating the number of steps.

0271–2091/81/010063–17$01.00 *Received 25 May 1980*

The effectiveness of the method is demonstrated on pure convection problems in one and two dimensions.

PROPERTIES OF THE SEMI-DISCRETE CONVECTION EQUATION

In this section we analyse the properties of the semi-discrete form of the convection equation with regard to the possible choices for mass representation: consistent or diagonal. For simplicity a uniform mesh of piecewise linear elements is assumed, but the conclusions of the analysis are easily extended to the case of linear isoparametric elements in two and three dimensions. The works of Krieg and Key[4] and Gresho *et al.*[1] are the basic guidelines for the present discussion.

To make it possible to compare the solution of the discrete equation to the solution of the differential equation, we consider the one-dimensional homogeneous model equation

$$\varphi_{,t} + u\varphi_{,x} = 0 \tag{1}$$

with constant u. If initial conditions are assumed in the form

$$\varphi(x, 0) = \hat{\varphi} e^{ikx} \tag{2}$$

the solution of equation (1) is

$$\varphi(x, t) = \hat{\varphi} e^{i(kx - \omega t)} \tag{3}$$

where $\omega = ku$ is the exact frequency.

On a uniform mesh of piecewise linear finite elements, the Galerkin formulation gives the following semi-discrete equation for the nodal value $\varphi_j(t)$:

$$(1 + rL)\dot{\varphi}_j + \frac{u}{2h}(\varphi_{j+1} - \varphi_{j-1}) = 0 \tag{4}$$

where $h = x_{j+1} - x_j$ and $L\varphi_j = \varphi_{j-1} - 2\varphi_j + \varphi_{j+1}$. The consistent mass results are obtained with $r = 1/6$ and the diagonal mass results with $r = 0$. Assuming a product solution for equation (4) in the form

$$\varphi_j = S_j . \psi(t) \tag{5}$$

separation of variables leads to the following pair of expressions

$$\beta(1 + rL)S_j + \frac{u}{2h}(S_{j+1} - S_{j-1}) = 0 \tag{6a}$$

$$\dot{\psi}(t) - \beta\psi(t) = 0 \tag{6b}$$

With initial conditions (2), equation (6a) indicates that β is given by

$$\beta = -i\omega \frac{\sin p/p}{1 + 2r(\cos p - 1)} \tag{7}$$

where $p = kh$ is a dimensionless wave number. The solution of equation (6b) is

$$\psi(t) = e^{\beta t} \tag{8}$$

and by analogy with the solution (3) to the exact differential equation (1) we rewrite equation (8) as

$$\psi(t) = e^{-i\bar{\omega}t} \tag{9}$$

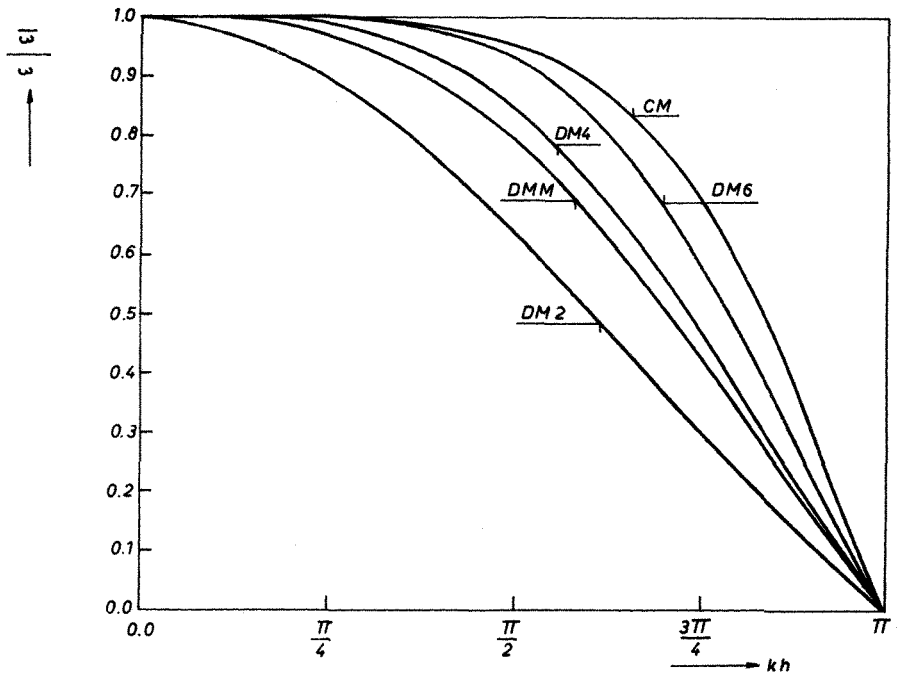

Figure 1. Ratio of semi-discrete frequency to exact frequency versus nondimensional wave number for a piecewise linear spatial approximation (CM: consistent mass; DM2: diagonal mass; DM4: 4th-order convection scheme; DM6: 6th-order convection scheme; DMM: intermediate scheme in equation (35))

If follows from equations (7)–(9) that the ratio of the semi-discrete frequency $\bar{\omega}$ to the exact frequency ω is given by

$$\frac{\bar{\omega}}{\omega} = \frac{\sin p/p}{1+2r(\cos p - 1)} \tag{10}$$

The dependency of the frequency ratio $\bar{\omega}/\omega$ on the dimensionless wave number p is shown in Figure 1 for $r = 1/6$ (consistent mass) and for $r = 0$ (diagonal mass). It appears that both the consistent and the diagonal mass representations depress the frequencies. The diagonal mass representation exhibits a particularly bad frequency response for intermediate and short wavelengths and this explains the poor performances of lumped-explicit schemes based upon linear elements in the solution of convection dominated problems.

HIGH-ORDER APPROXIMATIONS TO THE FIRST-ORDER SPATIAL DERIVATIVES

The deep frequency depression resulting from the diagonal mass representation is the direct consequence of a severe truncation error on the first-order spatial derivative. In fact, equation (4) with $r = 0$ indicates the spatial discretization based on piecewise linear elements yields a difference approximation to the convective term which is only second-order accurate:

$$\frac{\varphi_{j+1} - \varphi_{j-1}}{2h} = \left(\frac{\partial \varphi}{\partial x}\right)_j + \frac{h^2}{6}\varphi_j''' + O(h^4) \tag{11}$$

To improve the frequency response of lumped-explicit schemes based on linear elements, higher-order approximations to the first-order spatial derivative should be employed and these may easily be generated on using the following multistep explicit procedure which exploits the excellent phase characteristics of the consistent mass matrix without requiring its inversion:

— Suppose that the diagonal mass representation has been employed to derive a first approximation $\dot{\varphi}_j^{(1)}$ to the time derivative of the nodal values at a given time t. From equation (4) with $r=0$ we have

$$\dot{\varphi}_j^{(1)} = -\frac{u}{2h}(\varphi_{j+1}-\varphi_{j-1}) \tag{12}$$

— Now, using the consistent mass representation (equation (4) with $r=1/6$) we write

$$\tfrac{2}{3}\dot{\varphi}_j + \tfrac{1}{6}(\dot{\varphi}_{j-1}+\dot{\varphi}_{j+1}) = -\frac{u}{2h}(\varphi_{j+1}-\varphi_{j-1}) \tag{13}$$

and substituting $\dot{\varphi}_{j-1}$ and $\dot{\varphi}_{j+1}$ by their first approximation values in equation (12) we obtain a second approximation $\dot{\varphi}_j^{(2)}$ for the time derivative at node j in the form

$$\dot{\varphi}_j^{(2)} = -u\left[\frac{3}{2}\left(\frac{\varphi_{j+1}-\varphi_{j-1}}{2h}\right)-\frac{1}{2}\left(\frac{\varphi_{j+2}-\varphi_{j-2}}{4h}\right)\right] \tag{14}$$

— At this point, we note that a fourth-order accurate approximation to the first-order spatial derivative of φ may be obtained by linearly combining the approximations (12) and (14) in the form

$$\dot{\varphi}_j = (1-\alpha)\dot{\varphi}_j^{(1)} + \alpha\dot{\varphi}_j^{(2)} \tag{15}$$

which for $\alpha = 2/3$ gives

$$\dot{\varphi}_j = -u\left[\frac{4}{3}\left(\frac{\varphi_{j+1}-\varphi_{j-1}}{2h}\right)-\frac{1}{3}\left(\frac{\varphi_{j+2}-\varphi_{j-2}}{4h}\right)\right] \tag{16}$$

It is easily verified that the right-hand side of equation (16) represents a fourth-order accurate approximation to $\left(\dfrac{\partial\varphi}{\partial x}\right)_j$.

— If a sixth-order convection scheme is desired, we perform one more step and replace $\dot{\varphi}_{j\pm1}$ in equation (13) by the second approximation values in equation (14). This yields a third approximation $\dot{\varphi}_j^{(3)}$ which reads

$$\dot{\varphi}_j^{(3)} = -u\left[\frac{25}{16}\left(\frac{\varphi_{j+1}-\varphi_{j-1}}{2h}\right)-\frac{3}{4}\left(\frac{\varphi_{j+2}-\varphi_{j-2}}{4h}\right)+\frac{3}{16}\left(\frac{\varphi_{j+3}-\varphi_{j-3}}{6h}\right)\right] \tag{17}$$

We then combine the three approximations (12), (14) and (17) in the form

$$\dot{\varphi}_j = \tfrac{1}{15}\dot{\varphi}_j^{(1)} + \tfrac{2}{5}\dot{\varphi}_j^{(2)} + \tfrac{8}{15}\dot{\varphi}_j^{(3)} \tag{18}$$

and the result is

$$\dot{\varphi}_j = -u\left[\frac{3}{2}\left(\frac{\varphi_{j+1}+\varphi_{j-1}}{2h}\right)-\frac{3}{5}\left(\frac{\varphi_{j+2}-\varphi_{j-2}}{4h}\right)+\frac{1}{10}\left(\frac{\varphi_{j+3}-\varphi_{j-3}}{6h}\right)\right] \tag{19}$$

The right-hand side of equation (19) is an exact representation of $(\partial\varphi/\partial x)_j$ for a sixth-order polynomial.

— Generalizing the above results, it is concluded that on a uniform mesh of piecewise linear elements, the proposed multistep procedure may generate an approximation to the first order spatial derivative which is of order $2n$, n being the number of steps.
— It is also emphasized that the multistep algorithm is of purely explicit nature in the sense that it exploits the consistent mass matrix without requiring its inversion. In addition, the method can be readily extended to the basic isoparametric elements in two and three dimensions.

FREQUENCY RESPONSE OF THE HIGHER-ORDER SCHEMES

For the fourth-order accurate scheme in equation (16) the ratio of the semi-discrete frequency $\bar{\omega}$ to the exact frequency ω is given by

$$\frac{\bar{\omega}}{\omega} = \frac{4}{3}\frac{\sin p}{p} - \frac{1}{3}\frac{\sin 2p}{2p} \tag{20}$$

and it may be noted in Figure 1 that the frequency response is much better than that corresponding to the second-order convection operator obtained with the usual diagonal mass representation.

For the sixth-order approximation in equation (19), the frequency ratio is

$$\frac{\bar{\omega}}{\omega} = \frac{3}{2}\frac{\sin p}{p} - \frac{3}{5}\frac{\sin 2p}{2p} + \frac{1}{10}\frac{\sin 3p}{3p} \tag{21}$$

and Figure 1 indicates that a further significant improvement in frequency response is obtained with respect to the fourth-order convection scheme.

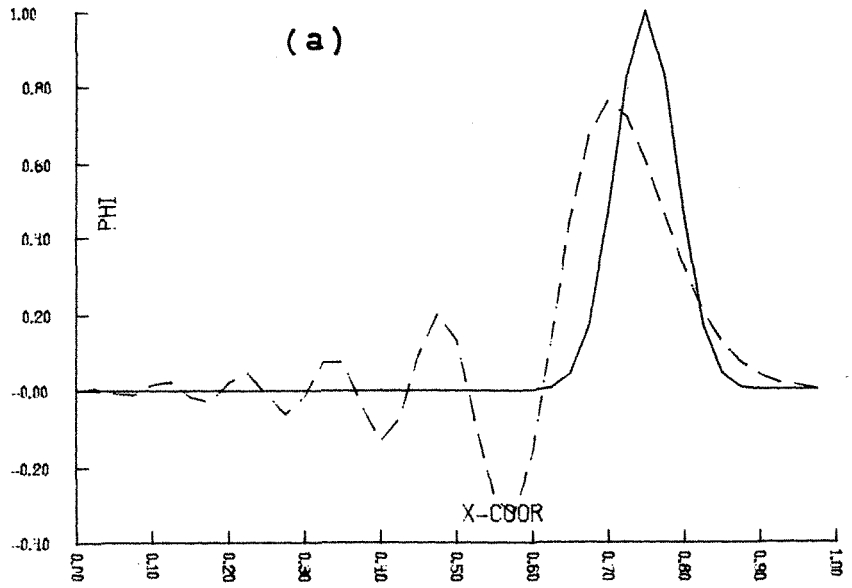

Figure 2. Pure advection of a Gaussian wave in one dimension: piecewise linear elements and leapfrog explicit time integration ($C = 0{\cdot}1$); (a) diagonal mass representation; (b) two-step explicit procedure; (c) three-step explicit procedure

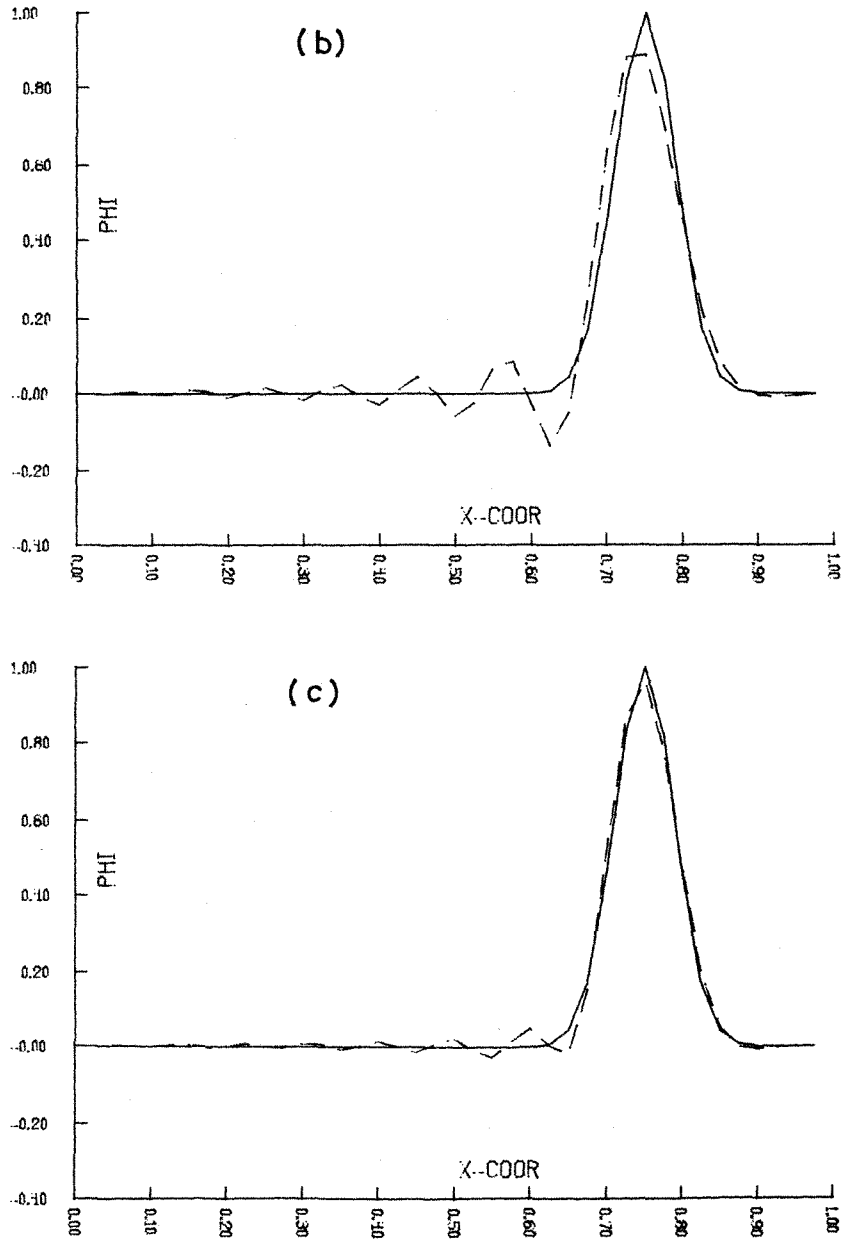

Figure 2. (*Continued*).

To illustrate the extent of improvement in accuracy obtained on using the proposed multistep explicit procedure, Figure 2 shows results for the pure advection of a Gaussian wave in one dimension. The temporal algorithm is the explicit leapfrog scheme with a Courant number $C = u\Delta t/h$ of 0·1, so that time truncation errors are virtually absent. The usual diagonal mass representation (second-order convection scheme) produces an important phase error which manifests itself by the presence of large spatial oscillations. These spurious

effects are already largely attenuated on using a two-step explicit procedure (fourth-order convection scheme) and when three steps are employed (sixth-order accurate scheme) the Gaussian wave is reproduced with a minimum of spurious oscillations.

EFFECTS OF EXPLICIT TIME INTEGRATION

To be cost-effective, explicit schemes must be operated at larger values of the Courant number than in the previous example and one should thus consider the effect of time discretization on the frequency response before any final judgement is made on the merits of lumped-explicit schemes based on linear elements.

Consider the time-centred leapfrog explicit scheme

$$\psi^{n+1} = \psi^{n-1} + 2\Delta t \psi'^{n} \tag{22}$$

and apply it to equation (6b) with $\beta = -i\bar{\omega}$. The result is

$$\psi^{n+1} + 2i\bar{\omega}\Delta t \psi^{n} - \psi^{n-1} = 0 \tag{23}$$

Equation (23) has a solution of the form

$$\psi^{n} = e^{-i\tilde{\omega} n \Delta t} \tag{24}$$

where the discrete frequency $\tilde{\omega}$ is given by

$$\sin \tilde{\omega}\Delta t = \bar{\omega}\Delta t \tag{25}$$

From equation (25) we note that the stability condition for the leapfrog explicit time integrator is

$$\bar{\omega}\Delta t \leqslant 1 \tag{26}$$

and that the ratio $\tilde{\omega}/\bar{\omega}$ is given by

$$\frac{\tilde{\omega}}{\bar{\omega}} = \frac{\sin^{-1}(\bar{\omega}\Delta t)}{\bar{\omega}\Delta t} \tag{27}$$

The frequency ratio $\tilde{\omega}/\bar{\omega}$ has been plotted in Figure 3 as a function of $\bar{\omega}\Delta t$ and it may be noted that the leapfrog explicit scheme has the effect of raising all of the semi-discrete frequencies $\bar{\omega}$. Now, comparing Figure 1 and Figure 3 one notes that compensating effects are obtained when combining a diagonal mass representation and an explicit time integration. Such effects will be analysed in detail in connection with the multistep explicit procedure discussed in this paper.

One-step explicit procedure

The one-step procedure corresponds to the usual diagonal mass representation and yields a second-order accurate convection operator as indicated by equation (12).

In view of equations (26) and (10) with $r = 0$, the stability condition for the leapfrog scheme is the familiar requirement

$$C = u\Delta t/h \leqslant 1 \tag{28}$$

where C is the Courant number.

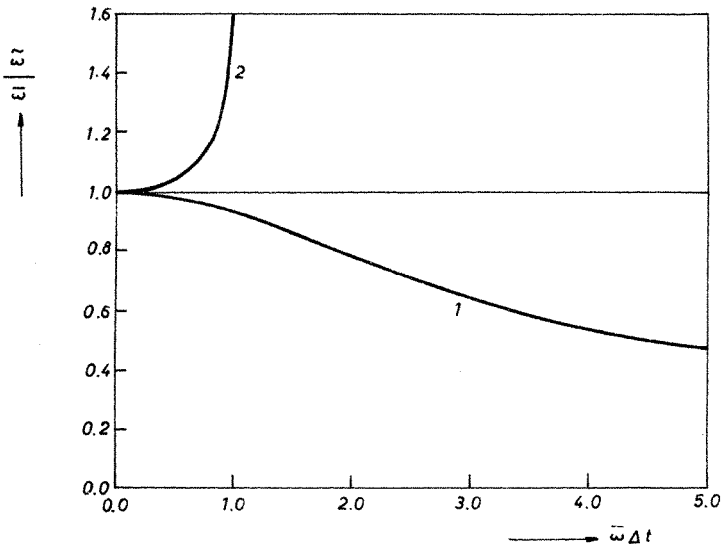

Figure 3. Frequency response for the implicit trapezoidal rule (1) and for the leapfrog explicit scheme (2)

From equations (27) and (10) with $r=0$, the ratio of the discrete frequency $\tilde{\omega}$ to the exact frequency ω is given by

$$\frac{\tilde{\omega}}{\omega}=\frac{\sin^{-1}(C\sin p)}{C\,.\,p} \tag{29}$$

One immediately notes from equation (29) that if the Courant number C is chosen as unity, the errors introduced by spatial discretization and numerical time integration exactly compensate and an exact frequency response is obtained for all wavelengths. However, in most practical situations it is not possible to operate at exactly the critical time step and the frequency response for lower values of the Courant number must be considered. The ratio $\tilde{\omega}/\omega$ in equation (29) has been plotted in Figure 4 as a function of the dimensionless wave number p for several values of the Courant number C. It appears that the strong frequency depression introduced by the diagonal mass representation cannot be adequately compensated by the opposite effect introduced by explicit time integration, unless the Courant number is taken very close to unity. The poor performances of explicit schemes based on simple mass lumping are confirmed by numerical experiments in one and two dimensions. Figure 5 shows results for the pure advection of a Gaussian wave in one dimension. The Courant number was varied between 0·2 and 0·8 and even for the largest value, the numerical answer is characterized by an excessive phase error. Figure 6 presents results for the standard problem[1–5] of the advection of a concentration cone in a pure rotation flow field. The exact solution (Figure 6(a)) consists of a rigid rotation of the cone about the centre of the mesh and it is noted that the numerical solution obtained on a uniform (30×30) mesh of bilinear elements exhibits a rather important phase error after one revolution of the cone (Figure 6(b)). The Courant number $u_{\max}\,.\,\Delta t/h$ was approximately 1·0, corresponding to a full 360-degree rotation of the cone in 100 time steps.

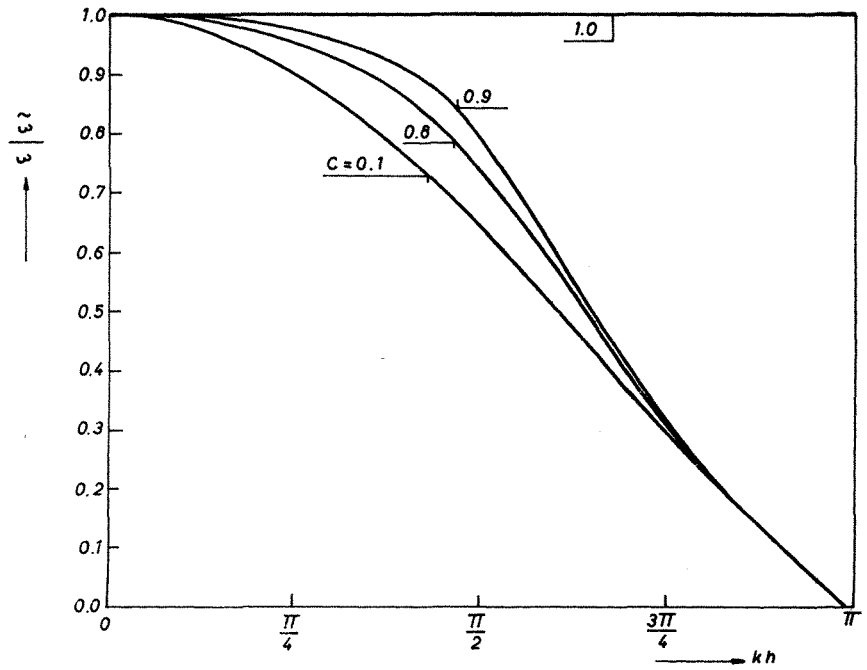

Figure 4. Ratio of computed frequency to exact frequency versus nondimensional wave number for leapfrog explicit time integration and diagonal mass representation. C is the Courant number

Two-step explicit procedure

As shown by equation (16), the two-step explicit procedure yields a fourth-order accurate convection operator and the stability condition for the leapfrog scheme is obtained from equations (26) and (20) in the form

$$\tilde{\omega}\Delta t = \frac{u\Delta t}{h} \cdot \text{Max}\left(\tfrac{4}{3}\sin p - \tfrac{1}{6}\sin 2p\right) \leqslant 1 \tag{30}$$

The corresponding limitation on the Courant number is found to be

$$C = \frac{u\Delta t}{h} \leqslant 0{\cdot}729 \tag{31}$$

To look at the effect on frequency response of combining the leapfrog scheme and a two-step diagonal mass representation, we consider the ratio of the discrete frequency $\tilde{\omega}$ to the exact frequency ω as obtained from equations (27) and (20):

$$\frac{\tilde{\omega}}{\omega} = \frac{\sin^{-1}\left[C\left(\tfrac{4}{3}\sin p - \tfrac{1}{6}\sin 2p\right)\right]}{C \cdot p} \tag{32}$$

It is noted from Figure 7 that the ratio $\tilde{\omega}/\tilde{\omega}$ becomes larger than unity for intermediate wavelengths if the Courant number is taken above a threshold value which is $C \simeq 0{\cdot}4$. It follows that for optimal accuracy the fourth-order convection scheme should be operated at

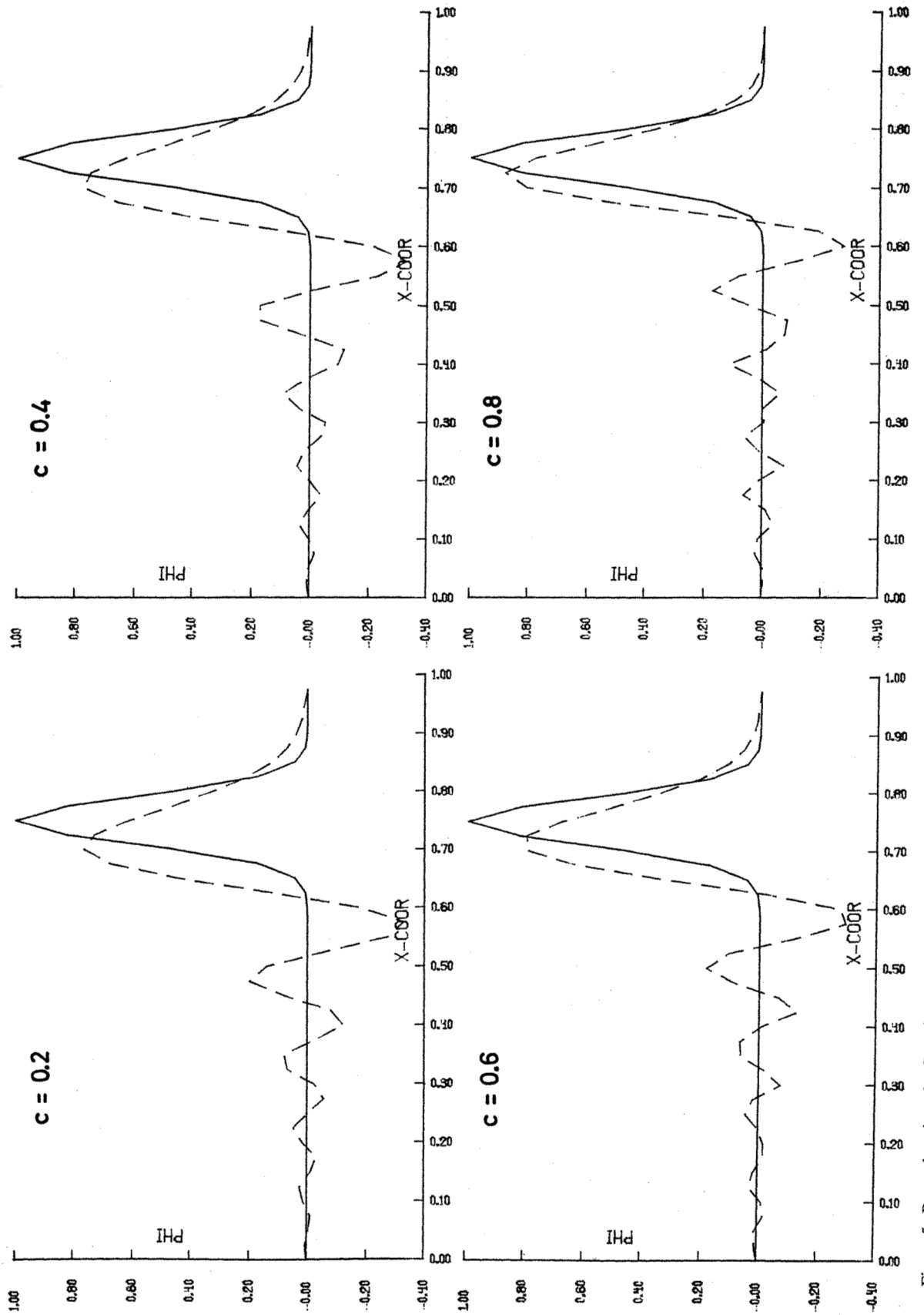

Figure 5. Pure advection of a Gaussian wave in one dimension: piecewise linear elements and leapfrog explicit integrator operated at different values of the Courant number C

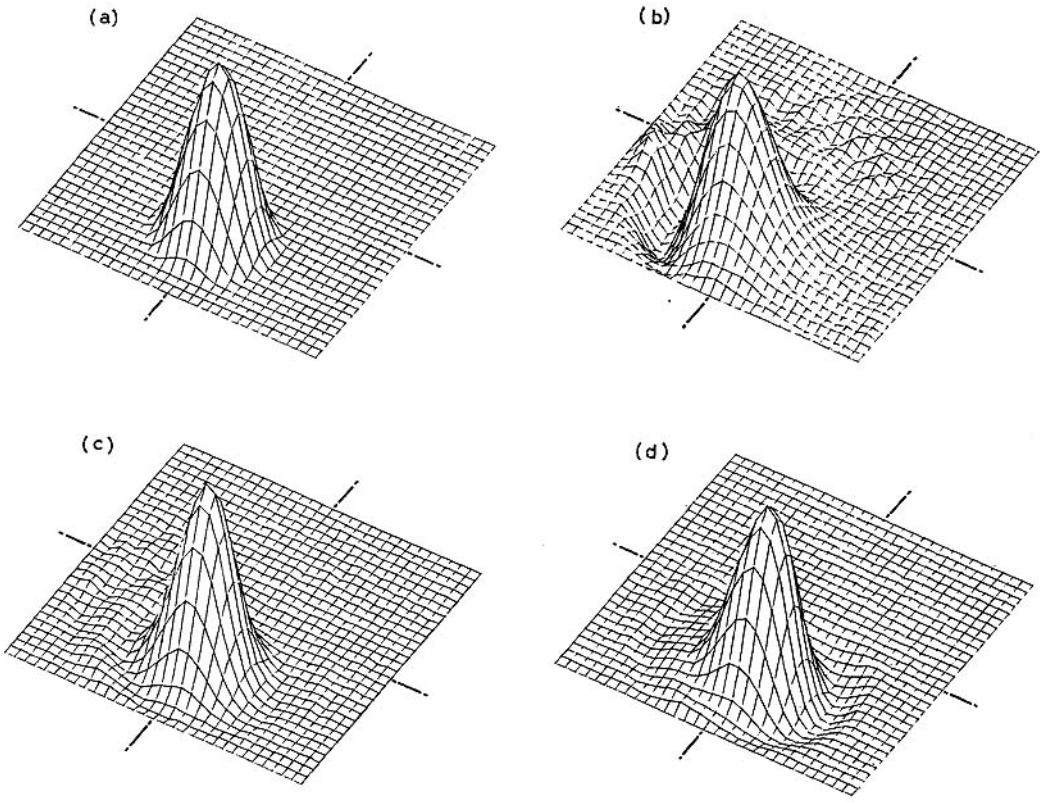

Figure 6. Advection of a concentration cone in a pure rotation flow field: results after one revolution. (a) exact solution; (b) diagonal mass representation ($C = 1{\cdot}0$); (c) intermediate convection scheme in equation (35) ($C = 0{\cdot}6$); (d) fourth-order convection scheme ($C = 0{\cdot}4$). C is the maximum Courant number

approximately the above value of the Courant number. This is confirmed by numerical experiments on the pure advection of a Gaussian wave as illustrated in Figure 8(a).

Three-step explicit procedure

As indicated by equation (19), the three-step explicit procedure produces a sixth-order accurate convection operator and the stability condition for the leapfrog time integrator derived from equations (26) and (21) is found to be

$$C = \frac{u\Delta t}{h} \leqslant 0{\cdot}631 \tag{33}$$

The ratio of the discrete frequency to the exact frequency is obtained from equations (27) and (21) in the form

$$\frac{\tilde{\omega}}{\omega} = \frac{\sin^{-1}\left[C(\frac{3}{2}\sin p - \frac{3}{10}\sin 2p + \frac{1}{30}\sin 3p)\right]}{C \cdot p} \tag{34}$$

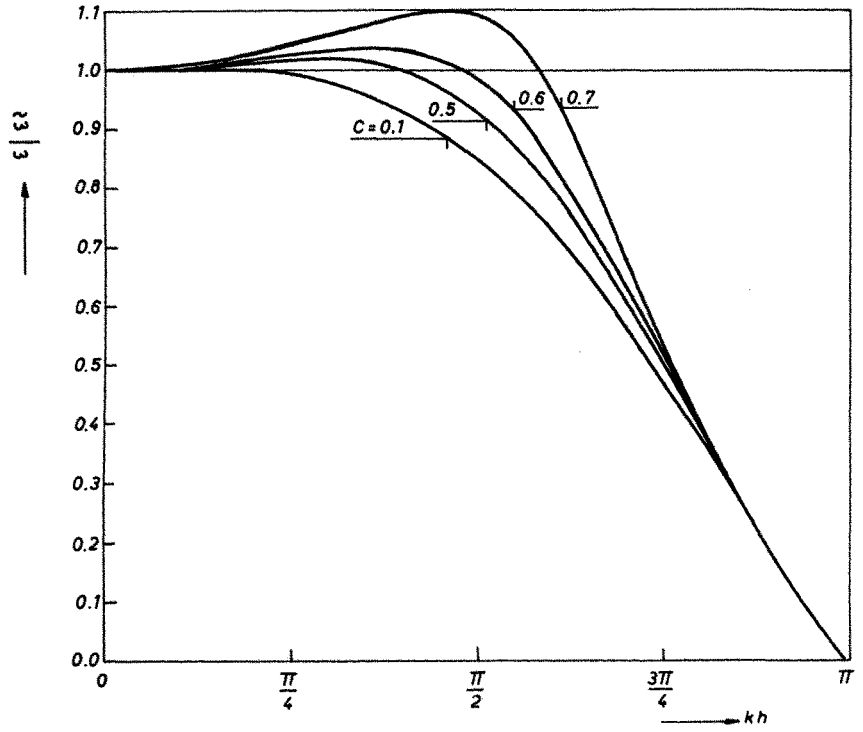

Figure 7. Ratio of computed frequency to exact frequency versus nondimensional wave number for leapfrog explicit time integrator and fourth-order convection scheme. C is the Courant number

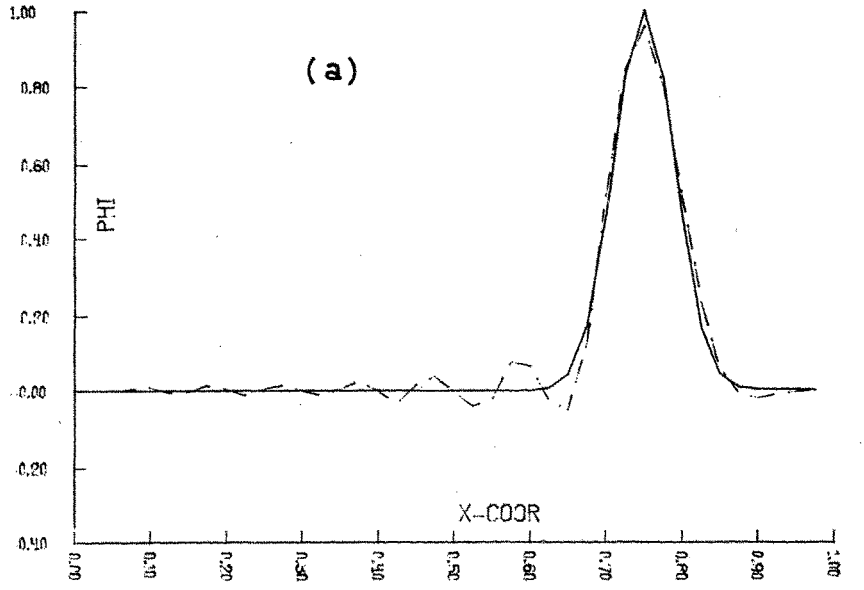

Figure 8. Pure advection of a Gaussian wave in one dimension: (a) fourth-order convection scheme and leapfrog integrator with $C=0.4$; (b) sixth-order convection scheme and leapfrog integrator with $C=0{\cdot}25$; (c) intermediate convection scheme in equation (35) and leapfrog integrator with $C=0{\cdot}6$

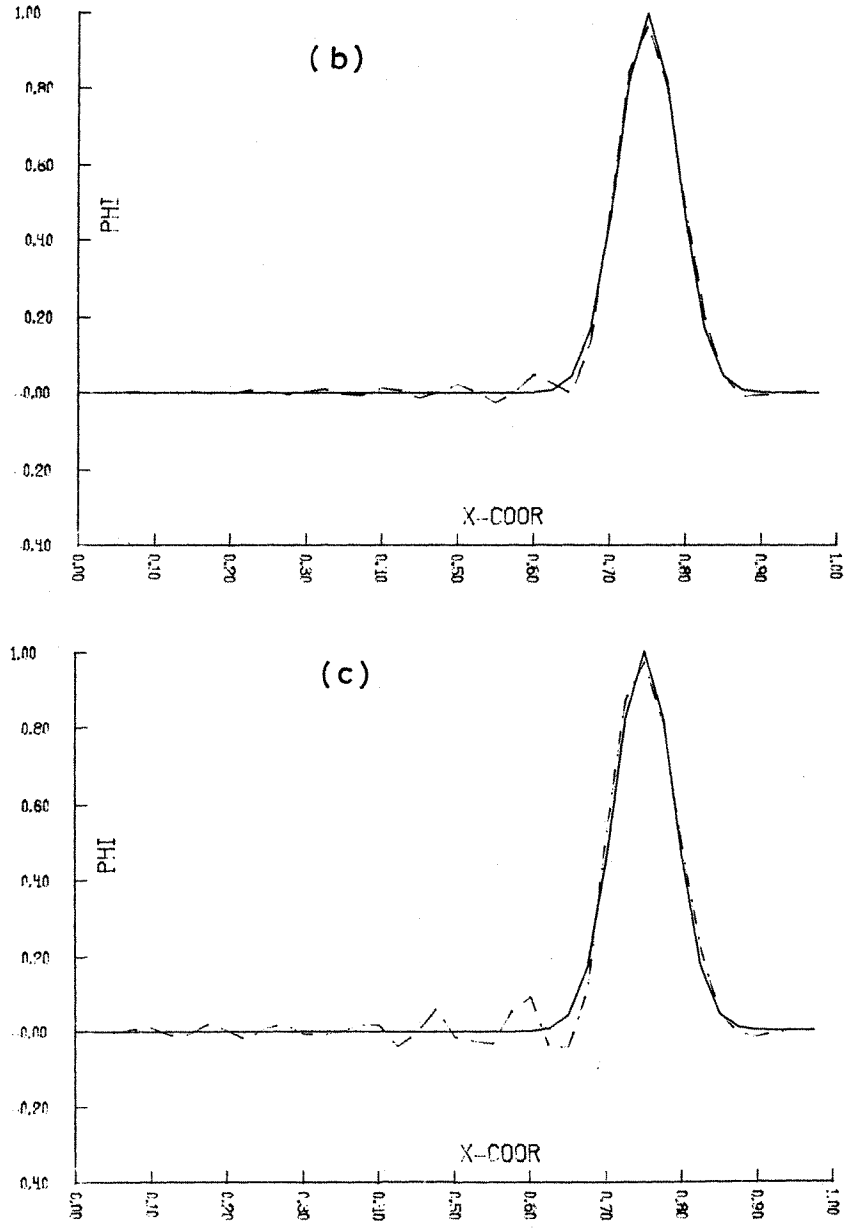

Figure 8. (*Continued*).

As shown in Figure 9, optimal accuracy is now obtained for a Courant number $C \simeq 0{\cdot}25$ and this is confirmed in Figure 8(b) where results are shown for the one-dimensional advection of a Gaussian wave.

A SCHEME WITH INTERMEDIATE SPATIAL ACCURACY

The following conclusions do arise from the discussion in the previous section:
— The usual diagonal mass representation produces a deep frequency depression that cannot

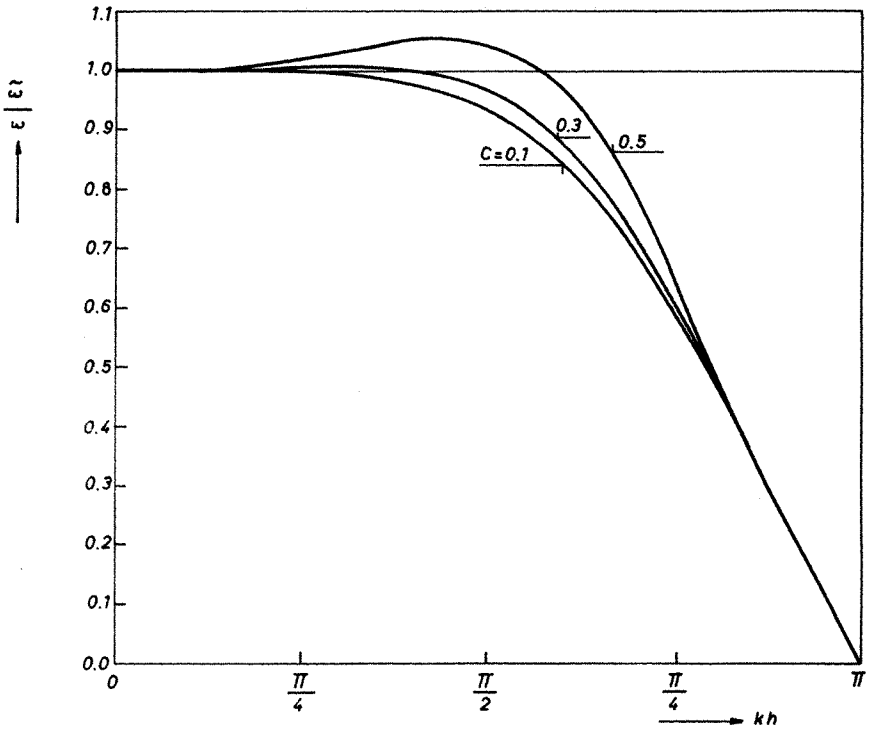

Figure 9. Ratio of computed frequency to exact frequency versus nondimensional wave number for leapfrog explicit time integrator and sixth-order convection scheme. C is the Courant number

be compensated by the opposite effect introduced by explicit time integration, even if relatively large values of the Courant number are employed.

— On the other hand, the higher-order convection schemes reduce the frequency depression to such an extent that, when combined with an explicit time integrator, this must be operated at rather small values of the Courant number to avoid an excessive phase lead for signals of intermediate wavelengths.

In these conditions, it appears that numerical results of acceptable accuracy could be produced on using larger time steps than permitted with the higher-order convection schemes if a scheme were devised with an accuracy intermediate between that of the second and the fourth-order operators. Consider for example[6] the intermediate scheme obtained on taking the arithmetic mean of the first two approximations (12) and (14), i.e. with $\alpha = 0{\cdot}5$ in equation (15):

$$\varphi_i = -u\left[\frac{5}{4}\left(\frac{\varphi_{j+1}-\varphi_{j-1}}{2h}\right)-\frac{1}{4}\left(\frac{\varphi_{j+2}-\varphi_{j-2}}{4h}\right)\right] \tag{35}$$

The resulting ratio of semi-discrete frequency $\bar{\omega}$ to exact frequency ω is shown in Figure 1 and the ratio of discrete frequency $\tilde{\omega}$ to exact frequency is plotted in Figure 10. It is seen that the intermediate scheme (35) behaves optimally when operated at a Courant number $C \simeq 0{\cdot}6$ and this is confirmed numerically in Figure 8(c) for the pure advection of a Gaussian

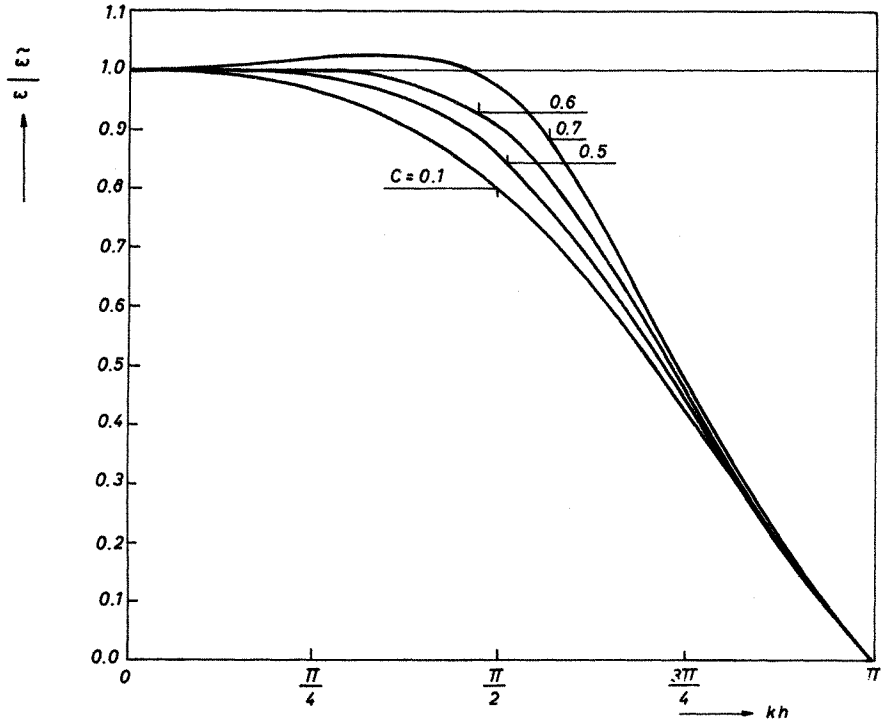

Figure 10. Ratio of computed frequency to exact frequency versus nondimensional wave number for leapfrog explicit time integrator and intermediate convection scheme in equation (35), C is the Courant number

wave. The stability condition for the leapfrog scheme is now

$$C \leqslant 0{\cdot}785 \tag{36}$$

In order to illustrate the extent of improvement in accuracy obtained on using the multistep explicit procedure for solving two-dimensional problems, we have treated the concentration cone problem on a uniform (30×30) mesh of bilinear elements. The results obtained with the intermediate scheme (35) are displayed in Figure 6(c); the Courant number $u_{\max} . \Delta t/h$ was approximately 0·6, corresponding to a full 360-degree rotation of the cone in 160 time steps.

Another calculation was made with the fourth-order convection scheme (16) operated at a Courant number of 0·4, corresponding to a full 360-degree rotation in 240 time steps. The results are displayed in Figure 6(d). With respect to the solution obtained with the usual mass lumping process, Figure 6(b), one notes that the amplitude of the trailing waves and the overall phase error have been considerably reduced in both higher-order calculations.

THE EXPLICIT/IMPLICIT QUESTION

Explicit time integration schemes do suffer from rather severe stability limitations but lead to an extremely simple computer program architecture. On the other hand, implicit methods are often unconditionally stable, but their algorithmic complexity may be a serious limitation,

especially in the presence of nonsymmetric and nonlinear convective terms. So there are good and bad possibilities with both categories of time integrators.

To further illustrate this point, consider the frequency response of the implicit trapezoidal rule

$$\psi^{n+1} = \psi^n + \frac{\Delta t}{2}(\dot{\psi}^n + \dot{\psi}^{n+1}) \tag{37}$$

applied to equation (6b) with $\beta = -i\bar{\omega}$. The result is

$$\psi^{n+1}\left[1 + i\frac{\bar{\omega}\Delta t}{2}\right] - \psi^n\left[1 - i\frac{\bar{\omega}\Delta t}{2}\right] = 0 \tag{38}$$

Equation (38) has a solution of the form indicated in equation (24) and the discrete frequency $\tilde{\omega}$ is now given by

$$\operatorname{tg} \tilde{\omega}\Delta t = \frac{\bar{\omega}\Delta t}{1 - \left(\frac{\bar{\omega}\Delta t}{2}\right)^2} \tag{39}$$

The ratio $\tilde{\omega}/\bar{\omega}$ is plotted in Figure 3 as a function of $\bar{\omega}\Delta t$ and it is noted that the implicit scheme (37) always reduces the semi-discrete frequencies $\bar{\omega}$. Since the consistent mass representation also depresses the frequencies (Figure 1), both time and space discretizations have the effect of reducing the frequencies. We are thus in the presence of what Krieg and

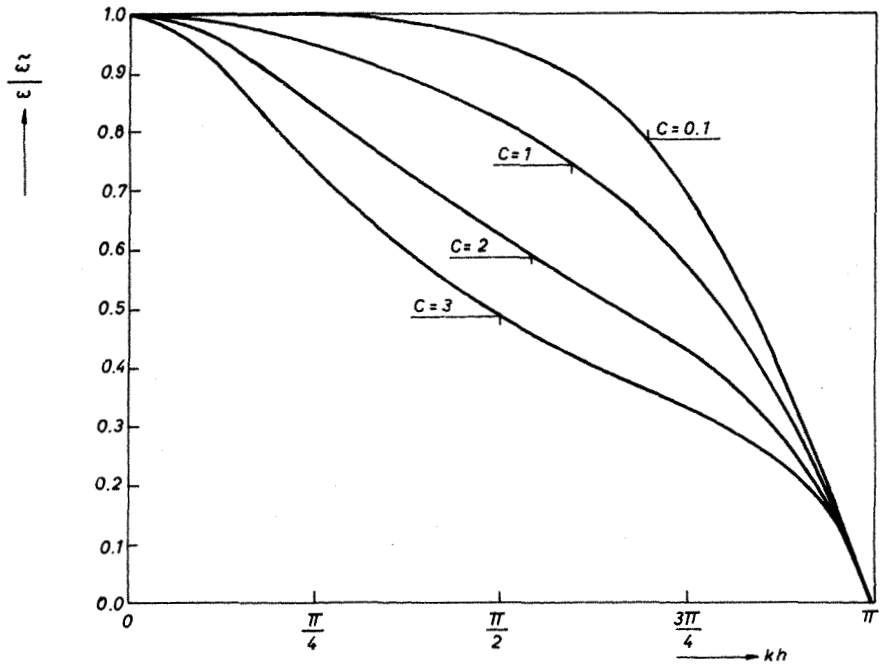

Figure 11. Ratio of computed frequency to exact frequency versus nondimensional wave number for the implicit trapezoidal rule, equation (37), and a consistent mass representation. C is the Courant number

Key[4] call an ill-matched method and a serious degradation in frequency response may be expected if large time steps are selected for implicit time integration. This is illustrated in Figure 11 where the ratio $\tilde{\omega}/\omega$ of the discrete frequency to the exact frequency is plotted as a function of the dimensionless wave number p for several values of the Courant number C. It is noted that a serious degradation in frequency response does appear if the implicit time integration scheme is operated at values of the Courant number larger than one. In these conditions, we prefer to take advantage of the algorithmic simplicity of the multistep explicit schemes discussed in the present paper. These should be particularly cost-effective in the solution of large-scale convection dominated problems in three dimensions.

CONCLUSIONS

A simple method has been presented which enables lumped-explicit schemes based on linear or multilinear finite elements to be endowed with phase characteristics that are much superior to those obtained with the usual diagonal mass representation. For optimal accuracy the size of the time increments for explicit time integration must be taken rather small, but it was also shown that only slightly larger time steps can be selected in conjunction with an implicit time integration scheme if an accurate frequency response is desired. It is therefore concluded that there may be good reasons for using explicit finite element algorithms in the numerical solution of convection dominated problems.

REFERENCES

1. P. Gresho, R. Lee and R. Sani, 'Advection-dominated flows with emphasis on the consequences of mass lumping', in *Finite Elements in Fluids*, Volume 3, Wiley, Chichester 1978.
2. J. Donéa, S. Giuliani and H. Laval, 'Accurate explicit finite element schemes for convective–conductive heat transfer problems', in *Finite Element Methods for Convection Dominated Flows* (Ed. T. J. R. Hughes), *AMD*, **34**, *ASME*, New York (1979).
3. S. I. Cheng, 'A critical review of numerical solution of Navier–Stokes equations', *Lecture Notes in Physics*, **41**, *Progress in Numerical Fluid Dynamics* (Ed. H. J. Wirz), Springer-Verlag, 1975.
4. R. D. Krieg and S. W. Key, 'Transient shell response by numerical time integration', *Int. J. num. Meth. Engng.* **7**, 273–286 (1973).
5. S. Orzag, 'Numerical simulation of incompressible flows within simple boundaries: accuracy', *J. Fluid Mech.*, **49**, 75 (1971).
6. J. Donea, S. Giuliani and H. Laval, 'Explicit finite element solution to transient convective–conductive heat transfer problems', *Proc. 1st Int. Conf. Num. Meth. in Laminar and Turbulent Flow*, Swansea, 17–21 July (1978).